

Nonlinear Aspects of the Evolution of Baroclinically Unstable Near-Surface Zonal Jets

F. J. Beron-Vera and M. J. Olascoaga

Division of Applied Marine Physics
Rosenstiel School of Marine & Atmospheric Science
University of Miami

Honolulu, 23 February 2006.

fberon@rsmas.miami.edu
www.rsmas.miami.edu/personal/fberon



Summary

We investigate finite-amplitude aspects of the evolution of baroclinically unstable zonal currents confined near the ocean's surface. We assume 2.5-layer QG dynamics on the β plane, which, possessing Lyapunov stable equilibria, allows one to derive upper bounds on growing perturbations using Shepherd's method.¹ Namely, bounds on baroclinic instability saturation as measured, e.g., in terms of the L_2 norm defined by the integral of layer enstrophies.

We improve the bound on zonally-averaged enstrophy variance derived using Shepherd's method by maximizing the latter subject to zonal momentum and layer enstrophies conservation. We further test the accuracy of the bounds by considering a finite-dimensional nonlinear (Hamiltonian) model that consistently approximates energy, zonal momentum, and layer entrophies (Casimirs) of the QG system. We find that the model admits solutions that maximize the enstrophy variance according to the rigorous bounds.

Infinite-Dimensional Dynamics

Let $(x, y) \in \mathbb{R}/L\mathbb{Z} \times [\pm W/2]$ on the β plane. Consider a 2.5-layer system with reference layer thicknesses $H/2$ and buoyancy jumps g' and g'/s (Fig. 1). The QG potential vorticity in the i th layer, $q_i(x, y, t)$, obeys

$$\partial_t q_i + [\psi_i, q_i] = 0, \quad (1a)$$

where

$$q_i = \beta y + \nabla^2 \psi_i + 2R^{-2}(\psi_{3-i} - \psi_i - \delta_{i2}s\psi_2). \quad (1b)$$

Here $[\cdot, \cdot]$ is the Jacobian bracket and $R := \sqrt{g'H}/|f_0|$.

Integrals of motion of (1) are energy, zonal momentum, and the generalized enstrophies (twice-infinite family of Casimirs):

$$\mathcal{E} := -\frac{1}{2} \sum \langle \psi_i q_i \rangle, \quad \mathcal{M} := \sum \langle y q_i \rangle, \quad \mathcal{C}_i^{(n)} := \langle q_i^n \rangle \quad (2)$$

(modulo Kelvin circulations along the coasts), where $\langle \cdot \rangle$ indicates horizontal average.

Furthermore, (1) constitutes a Lie–Poisson system since

$$\partial_t q_i = \{q_i, \mathcal{E}\}, \quad \partial_x q_i = \{\mathcal{M}, q_i\}, \quad 0 = \{q_i, \mathcal{C}_i^{(n)}\}, \quad (3)$$

where \mathcal{E} is the Hamiltonian and

$$\{A, B\} := \sum \left\langle q_i \left[\frac{\delta A}{\delta q_i'}, \frac{\delta B}{\delta q_i} \right] \right\rangle \quad (4)$$

is the Lie–Poisson bracket.

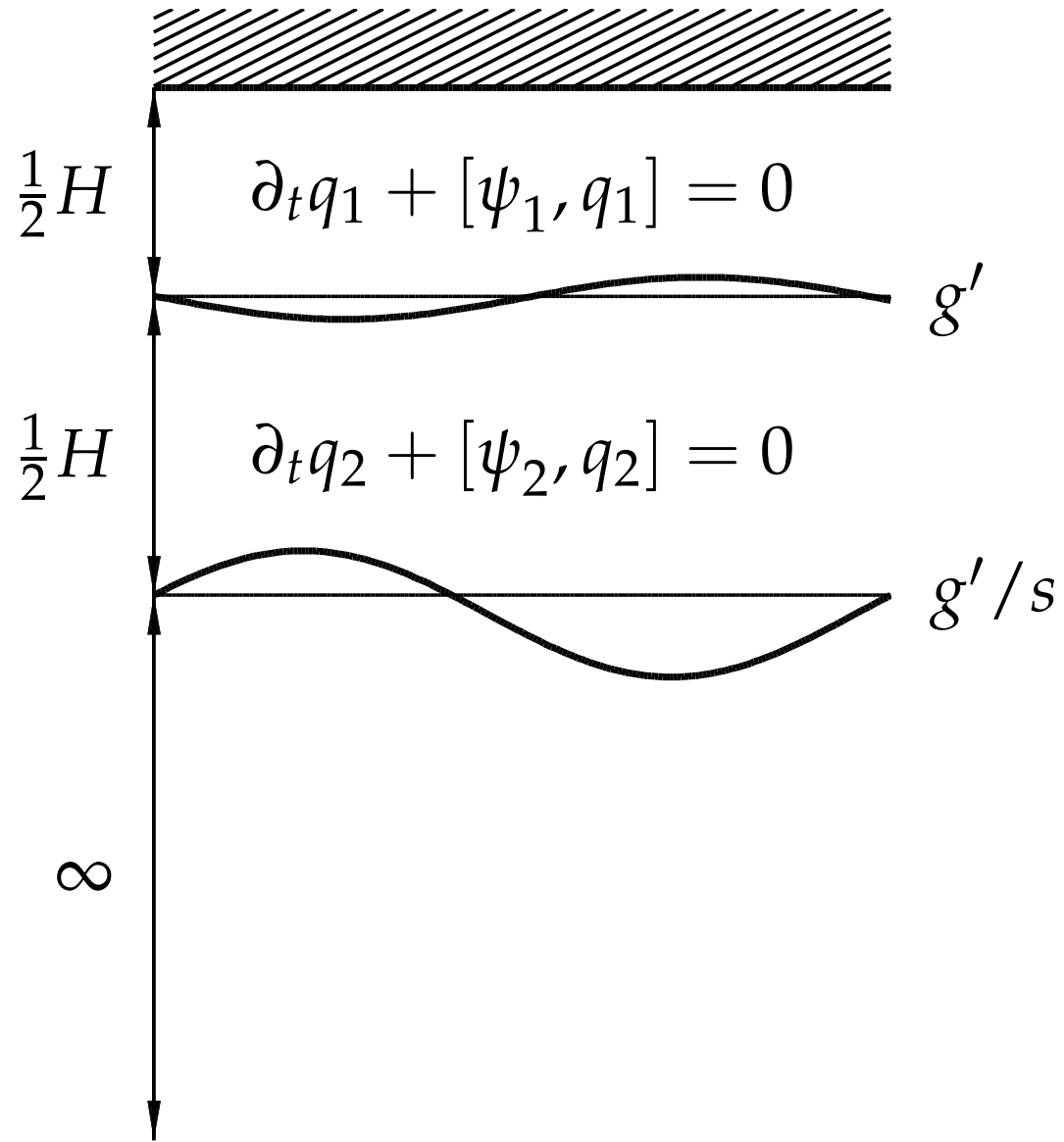


Figure 1. Model sketch.

Lyapunov Stability

Consider a basic state with uniform zonal currents U_i that differ in the vertical by $U_s := U_1 - U_2$ (Fig. 2). Then $Q_i(y) = Q'_i y$ with

$$Q'_1 = (1 + 2/b_P) \beta, \quad Q'_2 = (1 + 2(b_T - 1)/b_P) \beta \quad (5)$$

is a steady solution (i.e., equilibrium) of (1). Here

$$b_P := \beta R^2 / U_s, \quad b_T := s U_2 / U_s, \quad (6)$$

which are two Charney numbers.

An arbitrary perturbation $\delta q_i(x, y, t)$ on this state exactly satisfies

$$(\partial_t + \alpha \partial_x) \delta q_i = \{ \delta q_i, \mathcal{E}_p - \alpha \mathcal{M}_p \} \quad (7)$$

where

$$\mathcal{E}_p - \alpha \mathcal{M}_p = -\frac{1}{2} \sum \left\langle (U_i - \alpha) \delta q_i^2 / Q'_i + \delta \psi_i \delta q_i \right\rangle, \quad (8)$$

which is a combination of the pseudoenergy and pseudo-momentum.

It has been demonstrated² that if

$$(b_P, b_T) \in \{b_P < -2\} \cup \{b_P < 2 - 2b_T\} \quad (9)$$

then $\mathcal{E}_p - \alpha \mathcal{M}_p$ is positive definite and convex, which implies Lyapunov stability (Fig. 3).

Of particular interest here is that \mathcal{M}_p is sign definite and convex in the subset $|\lambda| > 1$ of (9), which implies

$$\frac{|\lambda| - 1}{|\lambda| + 1} \langle \delta \mathbf{q}^2 \rangle \Big|_{t=0} \leq \langle \delta \mathbf{q}^2 \rangle \leq \frac{|\lambda| + 1}{|\lambda| - 1} \langle \delta \mathbf{q}^2 \rangle \Big|_{t=0}, \quad (10)$$

where

$$\lambda := \frac{Q'_1 + Q'_2}{Q'_1 - Q'_2} \equiv \frac{b_P + b_T}{2 - b_T}. \quad (11)$$

Finally, a basic flow can be shown Lyapunov stable in the complement of (9) provided the zonal channel is narrow enough. More precisely, \mathcal{E}_p may be shown negative definite and convex.

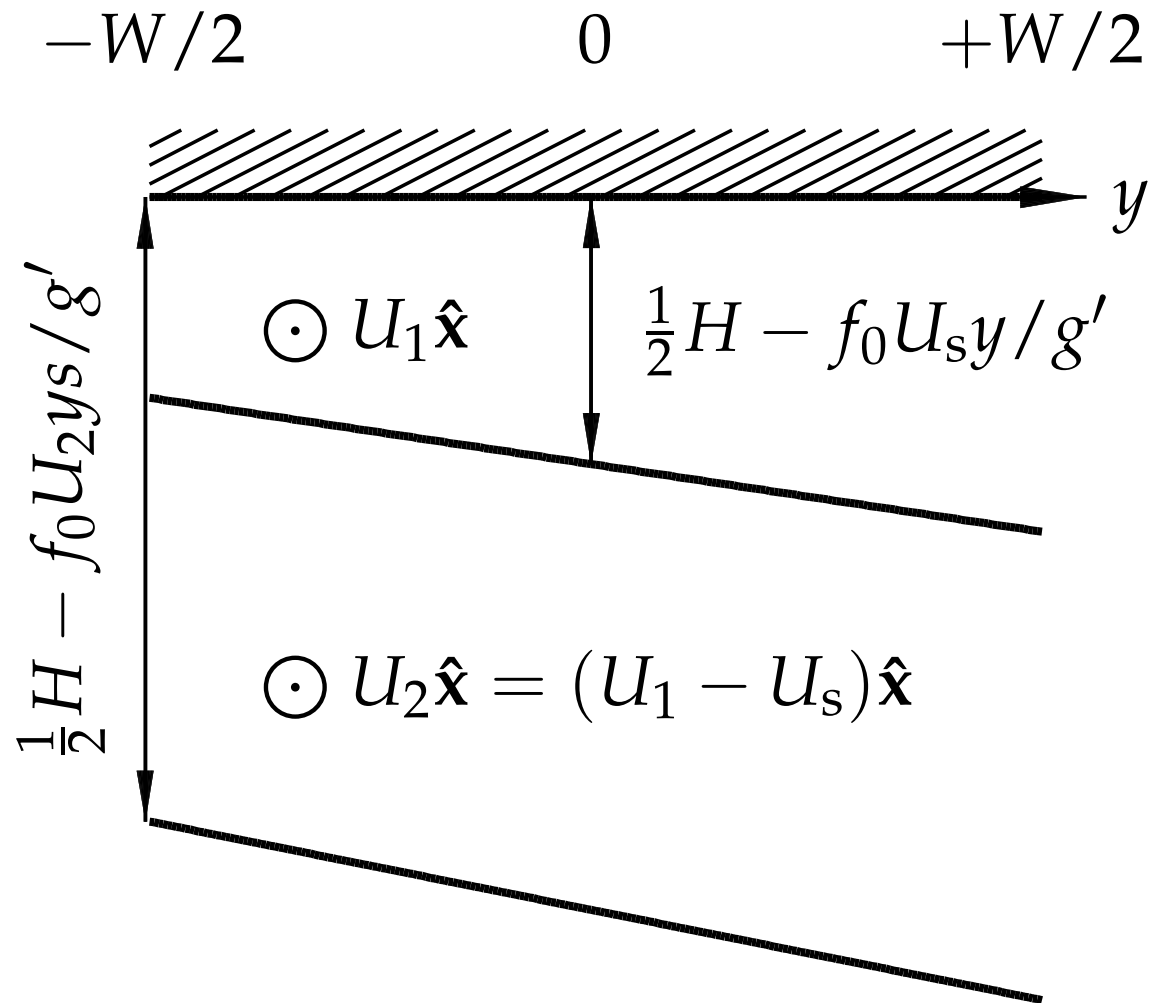


Figure 2. Basic state.

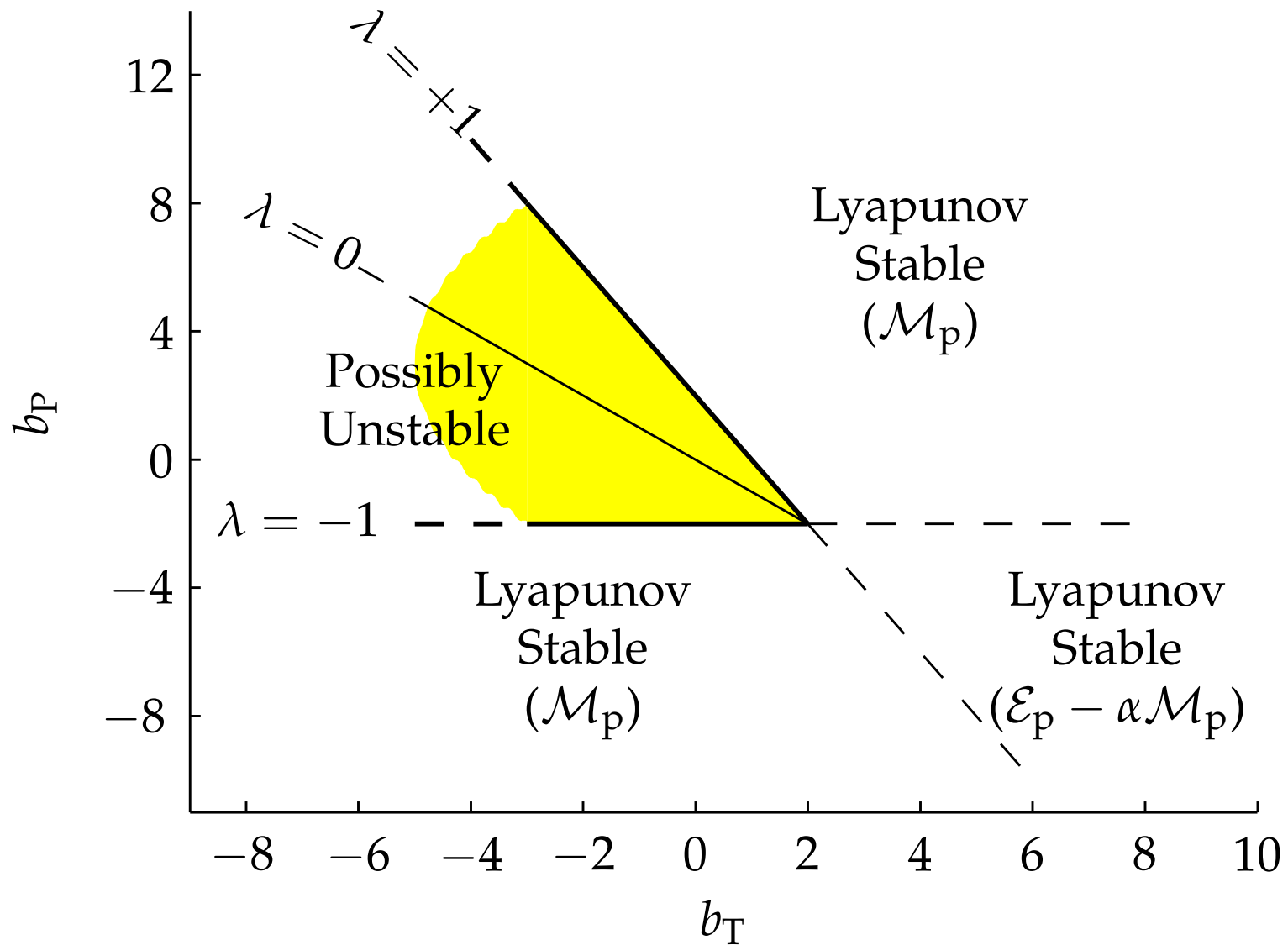


Figure 3. Regions of (in)stability in the topographic (b_T) vs. planetary (b_P) Charney numbers plane.

Bounds on Instability Saturation

Let $\mathbf{Q}(y)$ be an **unstable state**—which implies $|\lambda| < 1$ —and consider a perturbation to this state split as

$$\delta\mathbf{q}(x, y, t) = \delta\bar{\mathbf{q}}(y, t) + \delta\dot{\mathbf{q}}(x, y, t), \quad (12)$$

where $\delta\bar{\mathbf{q}}$ is a zonal average and $\delta\dot{\mathbf{q}}$ represents the “waves.” These quantities satisfy the Pythagorean relationship

$$\langle \delta\mathbf{q}^2 \rangle = \langle \delta\bar{\mathbf{q}}^2 \rangle + \langle \delta\dot{\mathbf{q}}^2 \rangle. \quad (13)$$

Let $\mathbf{P}(y)$ be a **stable state** with $|\lambda| > 1$ so that $\langle (\mathbf{q} - \mathbf{P})^2 \rangle$ is bounded according to (10). Assume that $\mathbf{q} \approx \mathbf{Q}$ at $t = 0$. Using the triangular inequality

$$\langle (\mathbf{q} - \mathbf{Q})^2 \rangle \leq \langle (\mathbf{q} - \mathbf{P})^2 \rangle + \langle (\mathbf{P} - \mathbf{Q})^2 \rangle, \quad (14)$$

and optimizing over \mathbf{P} , Shepherd's¹ method yield the least rigorous nonlinear bounds:²

$$\begin{array}{l}
|\lambda| \quad \langle \delta \bar{q}^2 \rangle / \langle Q^2 \rangle \quad \langle \delta \acute{q}^2 \rangle / \langle Q^2 \rangle \quad \langle \delta q^2 \rangle / \langle Q^2 \rangle \\
\leq \frac{1}{2} \left[\begin{array}{ccc} \frac{4(1 - |\lambda|)}{1 + \lambda^2} & \frac{1}{1 + \lambda^2} & \frac{4(1 - |\lambda|)}{1 + \lambda^2} \end{array} \right. \\
\geq \frac{1}{2} \left[\begin{array}{ccc} \frac{4(1 - |\lambda|)}{1 + \lambda^2} & \frac{4|\lambda|(1 - |\lambda|)}{1 + \lambda^2} & \frac{4(1 - |\lambda|)}{1 + \lambda^2} \end{array} \right.
\end{array} \quad (15a)$$

Using the method outlined below, however, the bound on $\delta \bar{q}$ (first column above) can be improved as

$$\frac{\langle \delta \bar{q}^2 \rangle}{\langle Q^2 \rangle} \leq \frac{4(1 - |\lambda|)^2}{1 + \lambda^2}. \quad (15b)$$

(Fig 4.).

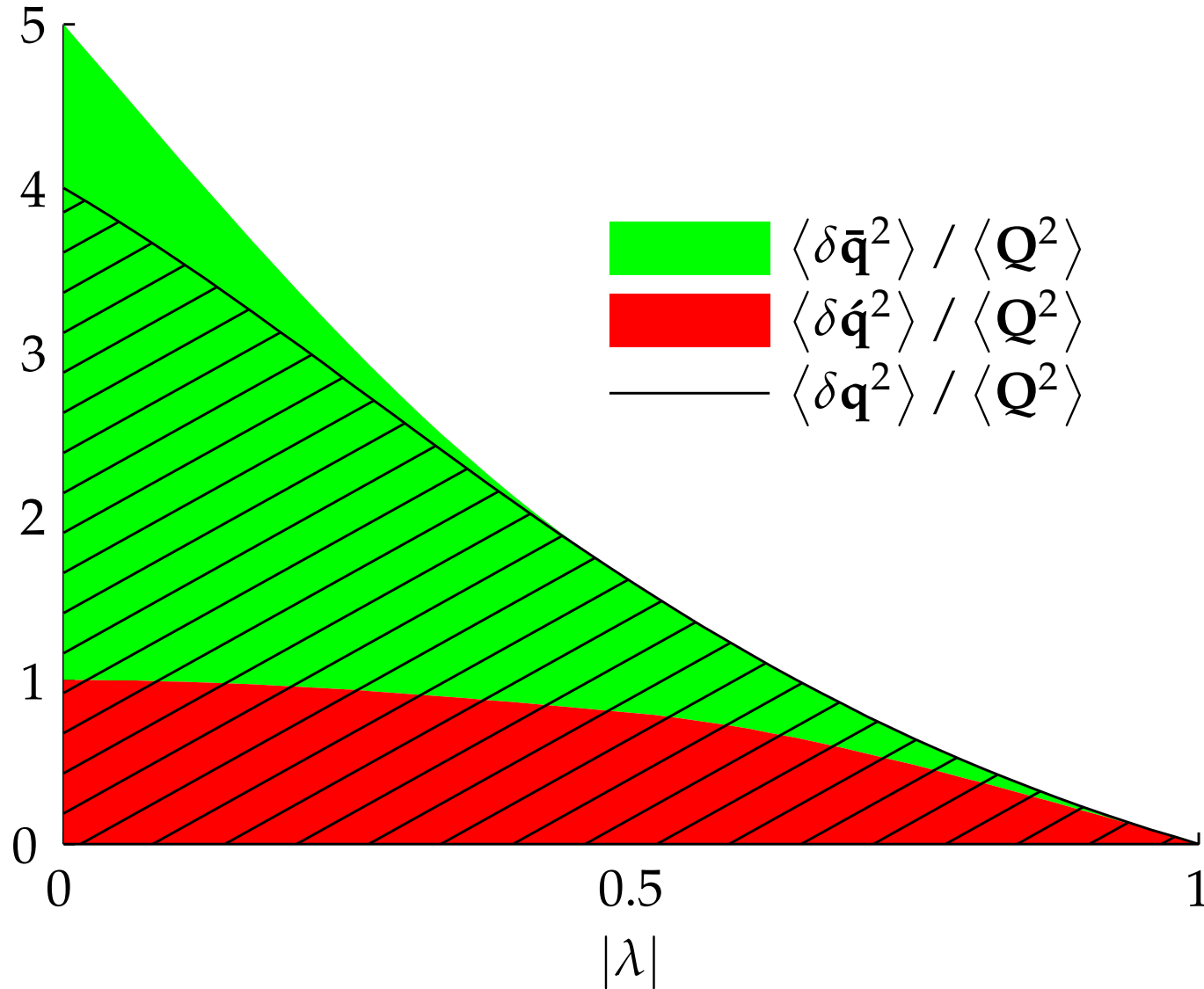


Figure 4. Rigorous nonlinear upper bounds on enstrophy variance(s). For slightly supercritical flows, $|\lambda| \downarrow 1$, the integrals of motion prevent the waves from growing. For $\lambda = 0$, the bound on $\delta \dot{\mathbf{q}}$ equals $\langle \mathbf{Q}^2 \rangle$ (total enstrophy of the system). Note that $\lambda = 0$ implies $b_P + b_T = 0$, which yields¹ the maximum normal-mode perturbation growth rate when $s \rightarrow 0$.

Derivation of Eq. (15b)

A priori bounds on baroclinic instability saturation can be formally obtained by maximizing

$$\begin{aligned} \Phi = \bar{v} \langle \delta \bar{q}^2 \rangle + \bar{v}' \langle \delta \dot{q}^2 \rangle \\ + \lambda (\mathcal{M} - \mathcal{M}|_{t=0}) \\ + \sum \lambda_i \left(c_i^{(2)} - c_i^{(2)} \Big|_{t=0} \right), \end{aligned}$$

where (\bar{v}, \bar{v}') equals either $(1, 0)$, $(0, 1)$ or $(1, 1)$.

Consider the Fourier expansions

$$\delta \bar{q}(y, t) = \sum_{n=1}^N \mathbf{A}_n(t) \sin nly, \quad (16a)$$

$$\delta \dot{q}(x, y, t) = \text{Re} \sum_{m,n=1}^{M,N} \mathbf{B}_{mn}(t) e^{imkx} \sin nly. \quad (16b)$$

Assuming an initial condition sufficiently close to the unsta-

ble state, conservation of \mathcal{M} is fulfilled by setting

$$\mathbf{A}_n = \begin{pmatrix} a_n \\ -a_n \end{pmatrix}. \quad (17)$$

On the other hand, conservation of $\mathcal{C}_i^{(2)}$ gives

$$\langle \delta \dot{q}_i^2 \rangle = \sum_{m,n} |B_{mn}^i|^2 = (-1)^{i-1} \sum_n l^{-1} Q'_i a_n - \frac{1}{2} a_n^2, \quad (18)$$

which sets bounds on a_n .

So we have

$$\langle \delta \bar{q}^2 \rangle = \frac{1}{2} \sum \mathbf{A}_n^2 \equiv \sum a_n^2, \quad (19a)$$

$$\langle \delta \dot{q}^2 \rangle = \sum \mathbf{B}_{mn}^T \mathbf{B}_{mn}^* \equiv \sum \frac{Q'_1 - Q'_2}{(-1)^n n l / 2} a_n - a_n^2, \quad (19b)$$

which, upon maximizing over a_n , yields the bounds (15a, center and left columns) and, in particular, (15b), all reduced by a factor

$$\frac{\sum_1^N n^{-2}}{\pi^2/6} \sim 1 \text{ as } N \rightarrow \infty. \quad (20)$$

Finite-Dimensional Dynamics

Following Ripa³ we consider

$$\delta\bar{q}(y, t) = \mathbf{A}(t) \sin 2ly, \quad \delta\dot{q}(x, y, t) = \text{Re } \mathbf{B}(t) e^{ikx} \sin ly, \quad (21)$$

where \mathbf{A} (real) represents mean flow changes and \mathbf{B} (complex) the waves (with zero zonal average).

Application of the methodology of Refs. 4,5 leads to amplitude equations in Hamiltonian form:

$$\dot{\mathbf{A}} = \{\mathbf{A}, \mathcal{E}_p\} = \{\mathbf{A}, \mathbf{B}\} \partial_{\mathbf{B}} E_p + \{\mathbf{A}, \mathbf{B}^*\} \partial_{\mathbf{B}^*} E_p, \quad (22a)$$

$$\dot{\mathbf{B}} = \{\mathbf{B}, \mathcal{E}_p\} = \{\mathbf{B}, \mathbf{A}\} \partial_{\mathbf{A}} E_p + \{\mathbf{B}, \mathbf{B}^*\} \partial_{\mathbf{B}^*} E_p, \quad (22b)$$

where

$$\{\mathbf{A}, \mathbf{B}\} = -2ikl \text{diag } \mathbf{B}, \quad (22c)$$

$$\{\mathbf{B}, \mathbf{B}^*\} = -2ikl \text{diag}(\mathbf{A} - l^{-1} \mathbf{Q}'), \quad (22d)$$

and

$$E_p := \frac{1}{2} \mathbf{A}^T \mathbf{E} \mathbf{A} + \text{Re } \mathbf{B}^T \tilde{\mathbf{E}} \mathbf{B}^* \quad (22e)$$

for certain (real and symmetric) matrices \mathbf{E} and $\tilde{\mathbf{E}}$.

System (22) supports two Casimirs:

$$\delta_{C_i}(\cdot) = \{C_i, \cdot\} = 0 \iff \boxed{C_i = \frac{1}{2}(A_i - Q'_i/l)^2 + |B_i|^2}. \quad (23)$$

Note that C_i consistently represents the i th-layer enstrophy $C_i^{(2)}$.

Integrals of motion of (22) also are

$$\delta_{E_p}(\cdot) = \{E_p, \cdot\} = -\partial_t(\cdot) \iff \boxed{E_p} \quad (24)$$

which consistently represents the pseudoenergy \mathcal{E}_p , and

$$\delta_M(\cdot) = \{M, \cdot\} = ik\mathbf{B}^T \partial_{\mathbf{B}}(\cdot) \iff \boxed{M = \frac{A_1 + A_2}{2l}} \quad (25)$$

which consistently represents the zonal momentum \mathcal{M} .[†]

*An explicit Lie algebra structure $\mathfrak{so}(3) \times \mathfrak{so}(3)$ shows up in the real coordinates $\{\mathbf{X}^a\}$ defined by $\mathbf{B} = \sqrt{2kl}(\mathbf{X}^1 + i\mathbf{X}^2)$ and $\mathbf{A} - l^{-1}\mathbf{Q}' = 2kl\mathbf{X}^3$: $\{\mathbf{X}^a, \mathbf{X}^b\} = (\varepsilon_c^{ab} \text{diag } \mathbf{X}^c)$ whose Casimirs are $\sum_a (X_i^a)^2$, $i = 1, 2$.

[†]Note that M is indeed the generator of infinitesimal zonal translations because $q_i(x, y, t) \rightarrow q_i(x + \varepsilon, y, t)$ corresponds to $\mathbf{A} \rightarrow \mathbf{A}$ and $\mathbf{B} \rightarrow \mathbf{B}e^{ik\varepsilon}$.

Furthermore, system (22) is **integrable**.³ This is readily seen by making the change of variables from *noncanonical* variables \mathbf{A} (real) and \mathbf{B} (complex) to canonical variables (a, A, θ, Θ) (real) in the form

$$A_i = A + (-1)^{i-1}a, \quad (26a)$$

$$B_i = (C_i - \frac{1}{2}(A_i - l^{-1}Q'_i)^2)e^{i(\Theta + (-1)^{i-1}\theta)}. \quad (26b)$$

Note that $\partial_{\Theta}E_p = 0$ and $\partial_A E_p = (\text{trace } \mathbf{E} + \mathbf{E}_{12})A$ so (A, Θ) constitute an action–angle pair. The orbits in the (a, θ) plane are the level curves of E_p for fixed C_i and A .

For $A = a(0) = 0$ and $|B_i(0)| \ll l^{-1}Q'_i$ (unstable state plus small wave) a trajectory in (θ, a) plane is closed and thus periodic: **a wave changes from riding on an unstable state to a stable state** (Fig. 5). Furthermore, all accessible orbits that collapse on the $a = 0$ axis, distinguished by $\theta(0)$, form a very thin set (solutions differ only by a time shift).

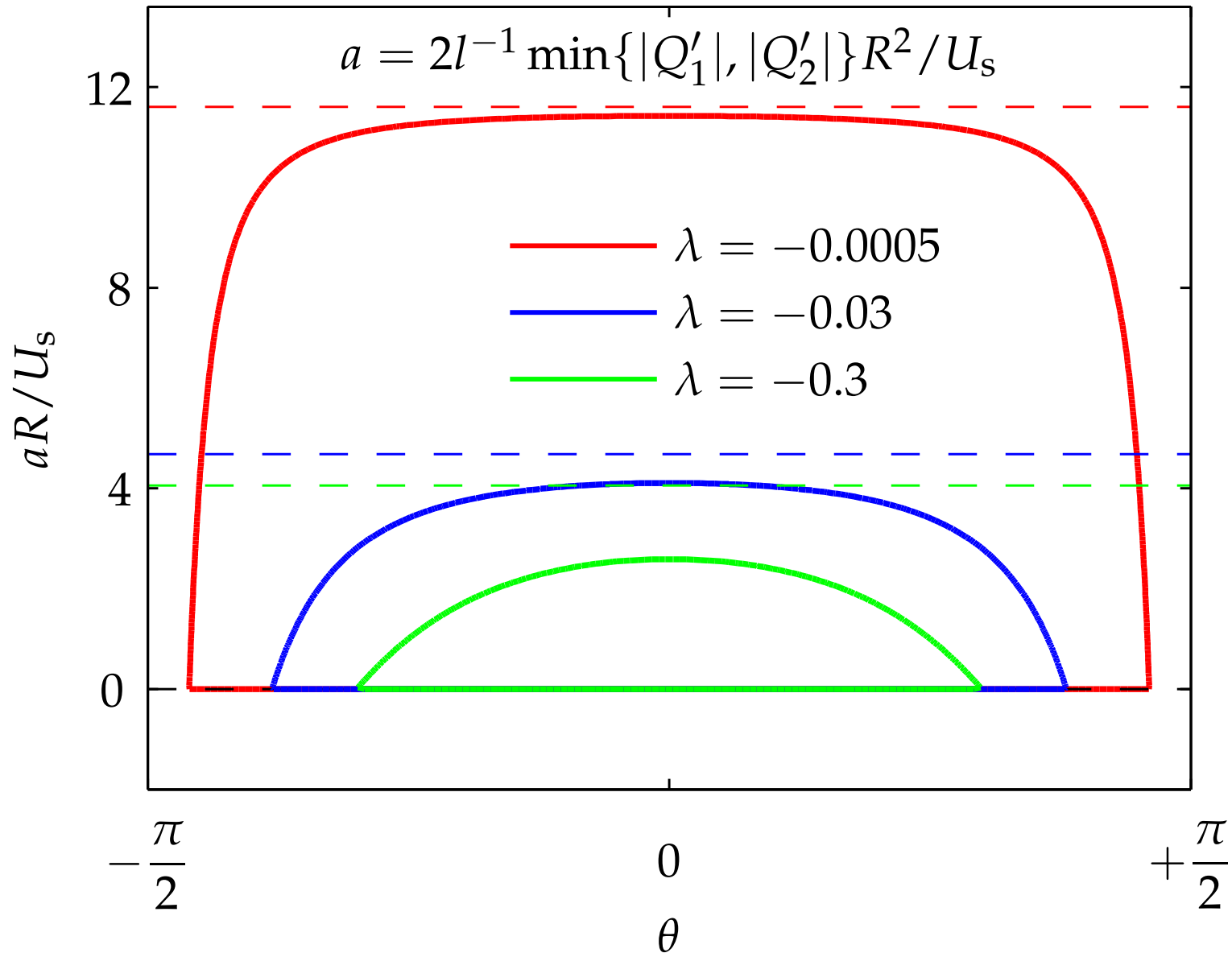


Figure 5. Contours of E_p for initial conditions close to different unstable states. Each contour corresponds to a trajectory describing a baroclinic periodic cycle: note that $\dot{a} \propto \sin 2\theta$ and $\dot{\mathbf{B}} = \mathbf{L}(a)\mathbf{B}$ where $\mathbf{L}(0)$ has real eigenvalues but $\mathbf{L}(a)$ has purely imaginary eigenvalues for a large enough.

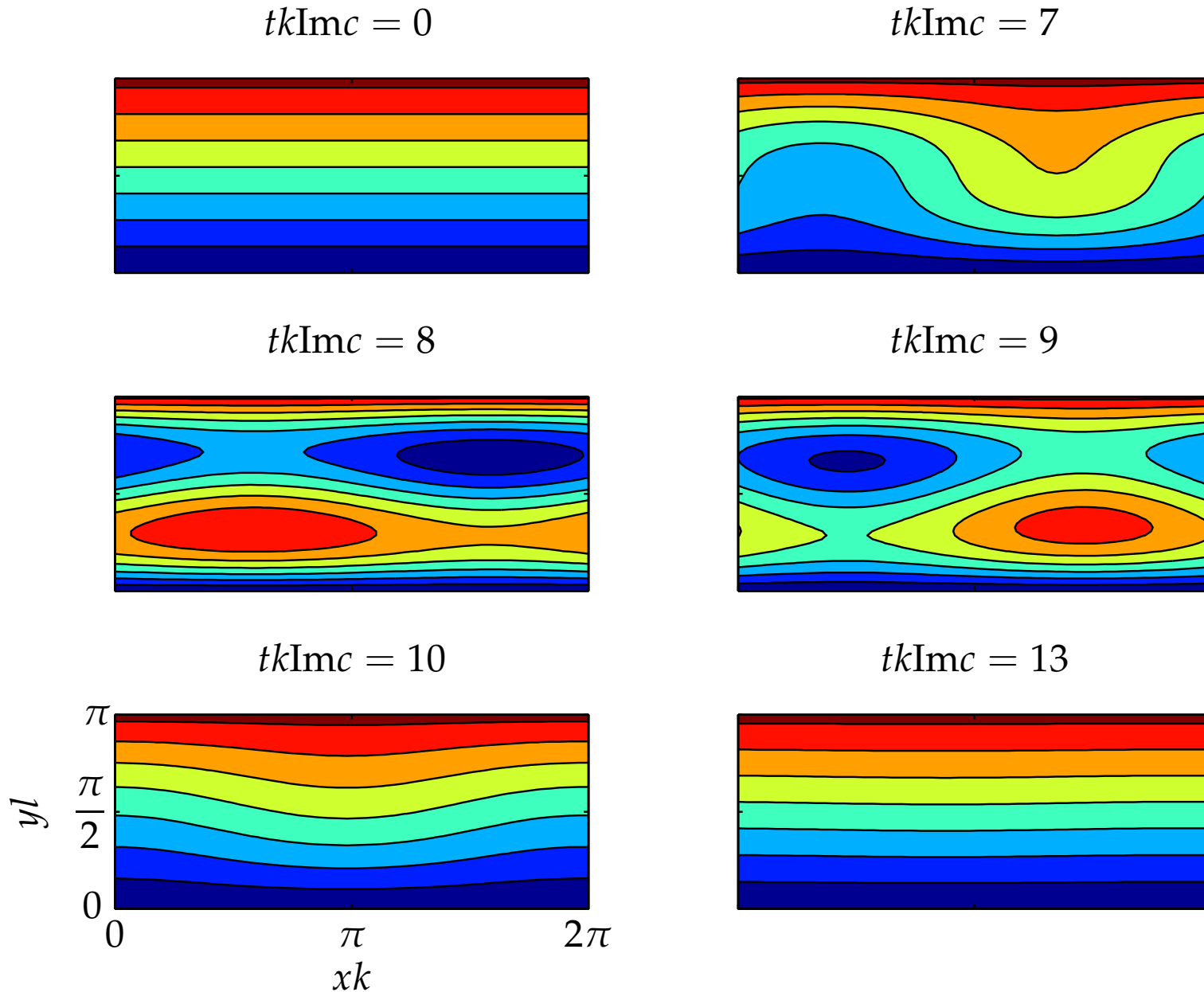


Figure 6. Evolution of potential vorticity in the upper layer as predicted by the finite-dimensional model (22). Shown are snapshots along one baroclinic cycle.

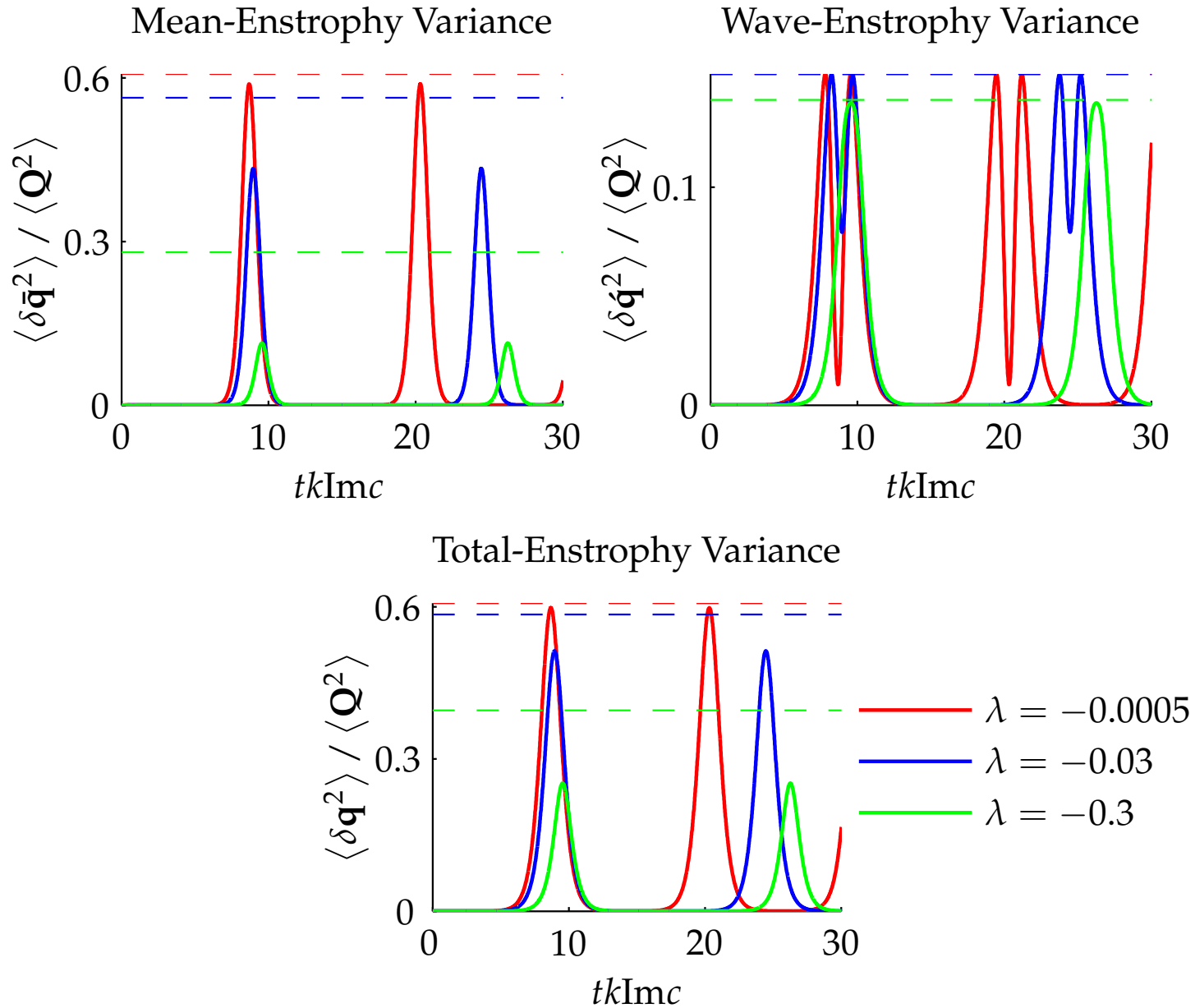


Figure 7. Evolution of enstrophy variance(s) as predicted by the finite-dimensional model (22) for several unstable states, each perturbed by the fastest growing normal mode. Dashed lines indicate a priori upper bounds on instability saturation, which are those in (15) reduced by a factor $3/2\pi^2 \approx 0.15198$.

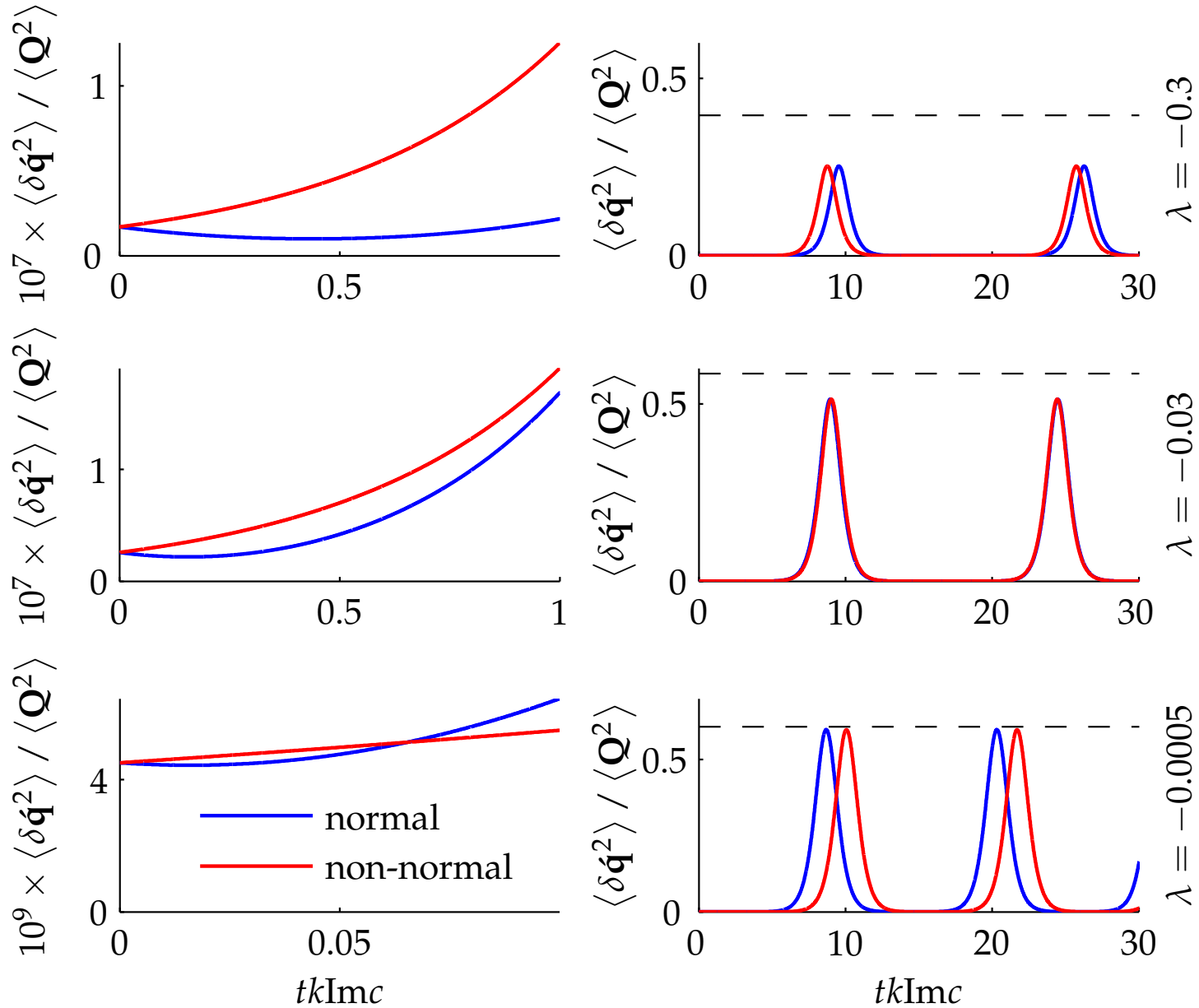


Figure 8. Evolution of total enstrophy variance as predicted by the finite-dimensional model (22) for several unstable states, each perturbed either by the fastest growing normal mode or the optimally growing non-normal mode. Dashed lines indicate a priori upper bounds on instability saturation.

Acknowledgement

Support for this work comes from NSF under grant CMG-0417425.

References

- ¹ T. G. Shepherd, *J. Atmos. Sci.* 45, 2014 (1988).
- ² M. J. Olascoaga and P. Ripa, *J. Geophys. Res.* 104, 23357 (1999).
- ³ P. Ripa, *Proc. 12th Conf. Atmos. Ocean. Fluid Dyn.*, p. 249, Am. Met. Soc. (1999).
- ⁴ S. P. Meacham, P. J. Morrison and G. R. Flierl, *Phys. Fluids* 9, 2310 (1994).
- ⁵ C. Scovel and A. Weisntein, *Com. Pure App. Math.* 47, 683 (1994).